Establishment and Theoretical Analysis of a Solar Driven NH_3-H_2O Resorption Heat Pump Cycle

Teng Jia, Yanjun Dai*

Institute of Refrigeration and Cryogenics, Shanghai Jiao Tong University, Shanghai (China)

Abstract

To make full utilization of low-temperature solar thermal, a novel balanced-type absorption-resorption heat pump (ARHP) cycle with a simple construction is proposed in this paper. The novel cycle is based on concentration difference of strong solution, weak solution and ammonia vapor (in fact a very small amount of water vapor inside). In order to achieve the optimal operating conditions, a mathematical model is developed and the feasibility and performance are investigated when factors like high and low generation pressure and ambient air temperature vary. Performance of the novel cycle is compared with that of the conventional single-stage absorption heat pump (AHP) cycle. The novel cycle is proved to have a smaller operation pressure differential compared to the conventional AHP cycle and is more suitable for the temperature characteristics of commonly used solar collectors. Coefficient of performance (COP) value of 1.42 can be obtained when high pressure (P_H) and low pressure (P_L) are respectively 1.40 MPa and 0.41 MPa under given working conditions. COP increases with the increasing of solar thermal temperature and ambient air temperature.

Key words: Solar thermal, absorption-resorption heat pump, simulation, COP

Nomenclature	
COP	coefficient of performance
PV	photovoltaics
AHP	absorption heat pump
GAX	generator–absorber exchanger (GAX)
FPC	flat plate collectors
ETC	evacuated tube collectors
HPG	high pressure generator
LPG	low pressure generator
HPA	high pressure absorber
LPA	low pressure absorber
SHX	solution heat exchanger
FRV	flow regulating valve
TV	throttling valve
Subscripts	
hpg	high pressure generator
lpa	low pressure generator
a	absorption
e	evaporation
c	condensation
H	high
L	low
h	heat source
lpg	low pressure absorber
hpa	high pressure absorber
*P*1	solution pump 1
m	mass flow rate [kg/s]
h	specific enthalpy [kJ/kg]
Q	heat exchanged [kW]
W	work, power [kW]
x	concentration [kg/kg]
T	temperature [°C]

doi:10.18086/swc.2017.28.10 Available at http://proceedings.ises.org

1, 2, …	state points
Greek symbols	
ξ	concentration [kg/kg]

1. Introduction

Heat pumps gain popularity by helping improve the quality of life by means of supplying heating in heating seasons and producing domestic hot water throughout the year. Improving their performance, reliability, and environmental impacts has been an ongoing concern (Chua et al. 2010). Conventional compression heat pumps are driven by electric power, and high-power compressors are often required to improve the performance (Fatouh and Elgendy 2011), which leads to many environmental problems. Solar energy is potential in driving heat pumps for different applications due to its cleanliness and accessibility (Fraga et al. 2015; Jradi et al. 2017; Zhou et al. 2016; Dai et al. 2015; Ozcan and Dincer 2013). Solar driven heat pumps can be divided into 3 kinds, i.e. heat pumps driven by thermal arrested by solar collectors, vapor compression heat pumps driven by solar photovoltaics (PV) and those combining solar thermal and vapor compression heat pumps. Among all the technical routes of solar driven heat pumps, the first kind has the highest solar thermal efficiency, which can theoretically convert 80% of the incident solar radiation energy into heating capacity. The combined heat pump systems use solar energy as the low-temperature heat source and are often combined with periodic heat storage devices to improve the cycle's COP by lifting the evaporation temperature (Omojaro and Breitkopf 2013). Electricity is still the basic power source for winter heating. Wu et al. (2014a, 2014b) reviewed recent absorption heating technologies and ammonia-based absorption heat pumps and pointed out that vapor compression and resorption heat pumps were suitable for wider temperature range than absorption ones. Van de Bor D. M. et al. (2014) numerically investigated many compression-resorption heat pumps with ammonia-water as working fluid for 50 specific industrial cases. The simulation results showed that the optimal performance, along with the lowest compression power and reduced investment and operating costs, is obtained under conditions which make the quality of vapor into the resorber be exact 100%. In practice, the vapor quality cannot reach 100% and compressors often work in the wet compression regime with a lower isentropic efficiency. Limited by cycle modes and high driven temperature, these products didn't utilize solar energy. Velázquez N. et al. (2002) presented a methodological analysis and energy evaluation of an air-cooled ammonia–water absorption heat pump with a generator–absorber heat exchanger (GAX) and operated by a hybrid natural gas–solar energy source. The heat pump allowed 19% of solar contribution at full load. A COP value of up to 1.86 was calculated by using ambient air up to 40°C with a relative humidity of 24% as cooling source. The system had a working pressure difference of up to 1.50 MPa and must be equipped with a rectifier. The required temperature of heat source is up to 150 °C, making function time of solar thermal relatively short, which together with the complex structure and high investment cost limited its application.

An absorption-resorption heat pump is formed when the evaporator and condenser in a conventional absorption heat pump are displaced by a low-pressure generator and a high-pressure absorber, respectively, and it completes the inner cycle relying on the concentration difference change of the binary mixtures. Although solar energy utilization is plagued by its intermittence and volatility, absorption-resorption heat pumps are still viable alternatives to supply winter heating in low-temperature environment when utilizing proper working fluid and high-temperature heat sources. Moreover, efficient and stable heating can be achieved by capacity regulating, energy complementary and working fluid storage, making solar driven absorption-resorption heat pump a research hotpot in the field of solar heating worldwide. Du et al. (1991, 1993) analyzed an unbalanced type of absorption -resorption heat pump with ammonia-water as working fluid. The simulation results showed that the system's highest working pressure is determined by the ammonia concentration in the cycle. The cycle appeared stronger adaptability to the environment by regulating ammonia concentration under varying operating conditions. The system was equipped with two solution pumps and the required temperature of generating is too high for efficient application of solar thermal.

This paper presents a novel balanced-type ammonia-water absorption-resorption heat pump which can be driven by solar thermal of lower temperature and of wider temperature range than the abovementioned GAX ones and the unbalanced types, which makes it possible to use flat plate collectors (FPC) and evacuated tube collectors (ETC).

As depicted in Fig. 1, in a conventional AHP cycle, concentration of solution out from condenser is 100%, while in a balanced ARHP cycle, outlet solution concentration of HPA is lower than 100%. Therefore, given the same temperature of solutions out from HPA and condenser, P_H of the novel cycle is lower than that of a conventional AHP cycle (ΔP_H), consequently resulting in a temperature decline of ΔT_h at the generator side, which makes it possible to utilize low-temperature heat source to drive ARHPs for space heating. Besides, given the same inner pressure difference in the two types of heat pumps, a pressure difference (ΔP_L) can also be achieved between evaporator and LPG. "Balanced" here means that there is overlap between the solution concentration range of the left and right sub-cycle Solution streams out from LPG and LPA are mixed together and then pumped to HPA and HPG to complete high-pressure absorption and generation process, respectively.

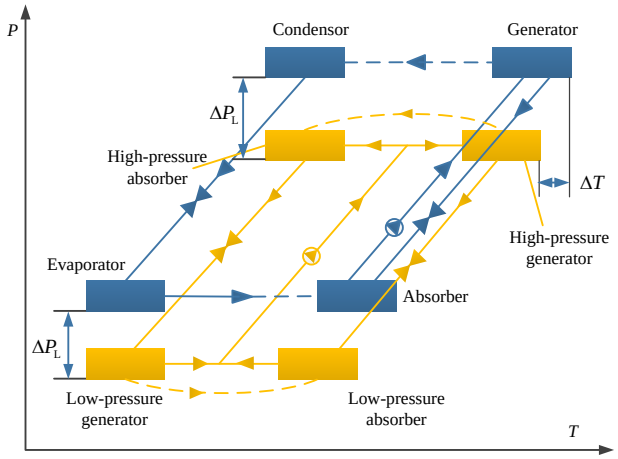

Fig. 1: Comparison of the conventional AHP cycle and the ARHP cycle proposed in this paper

2. Cycle description

The schematic diagram of the proposed balanced ARHP cycle is shown in Fig. 2. The pressure-temperature ($P-T$) diagram of the aqueous ammonia is shown in Fig. 3. The novel cycle comprises the following main components: HPG (high pressure generator), SHX1, 2 (solution heat exchanger 1, 2), TV1, 2 (throttling valve 2), LPA (low pressure absorber), solution mixing tank (SMT), P1 (solution pump1), solution separation tank (SST), HPA (high pressure absorber), LPG (low pressure generator). In order to clarify different heat absorption processes in low pressure generator, LPG is functionally divided into two parts, LPG1 which takes heat from the ambient and LPG2 which recovers heat from warm solution out from HPA. Ammonia/water is utilized as working pair in this work. The working principle is detailed as follows.

1-2-3-4-5-6-7-8-9-1 is a closed solution circuit. The weak solution out from HPG (1) is precooled by the solution out from SHX1 to state point (2) and then throttled in TV2 to low-pressure (P_L) (3). The solution (3) then absorbs the vapor (16) from LPG, releasing the absorption heat and becoming strong solution (4). The strong solution discharged from LPA (4) is then blended in the SMT with the solution (5) from LPG to make solution (6). The solution (6) is preheated in SHX2 by the hot solution from HPG to solution (7). The solution (7) is pressurized through P1 to high-pressure solution (8). Solution (9) (a portion of solution (8)) then enters HPG and heated by solar thermal to generate, making high-temperature and high-pressure vapor (17/18) and weak solution (1). The solution circuit of the right sub-cycle is finished.

15-6-7-8-9-10-11-12-13-14-5 is another solution circuit. The weak solution out from LPA (5) (which is stronger than the solution (1)) is blended in the solution mixing tank with the solution out from LPA (4) into the solution (6). The solution (6) is then preheated in SHX2 by the solution (1) out from HPA to (7). The solution (7) is pressurized through P1 to high-pressure solution (8). Solution (10) (the remaining portion of solution (8)) then enters LPA and absorb the vapor (18/17), giving off the resorption heat and forming strong solution (which is stronger than solution (4)). The strong solution out from HPA (11) is precooled by solution (14) in LPG2 to solution (12). The high-pressure solution (12) is then depressurized by TV1 to low-pressure solution (13). The low-temperature solution (13) then enters LPG and takes heat from the ambient to

generate, discharging low-temperature and low-pressure vapor in turn in LPG1 and LPG2 and making weak solution (5) (which is stronger than solution (1)). The solution circuit of the left sub-cycle is finished.

t should be pointed out that the amount of solution (4) and solution (9) are not the same due to the different amount of vapor (17/18) and (16). In the same way, the amount of solution (14) and solution (10) are different.

17-18 and 15(15a)-16 are the high- and low-pressure ammonia vapor flow, respectively. 23-24 is the ambient air flow acting as the low-temperature heat source. 19-20-21-22 is the series supply/return water flow. 25-26 is the working medium out from/ into solar collectors, which serves as the high-temperature heat source (80~100 ^{o}C in this paper).

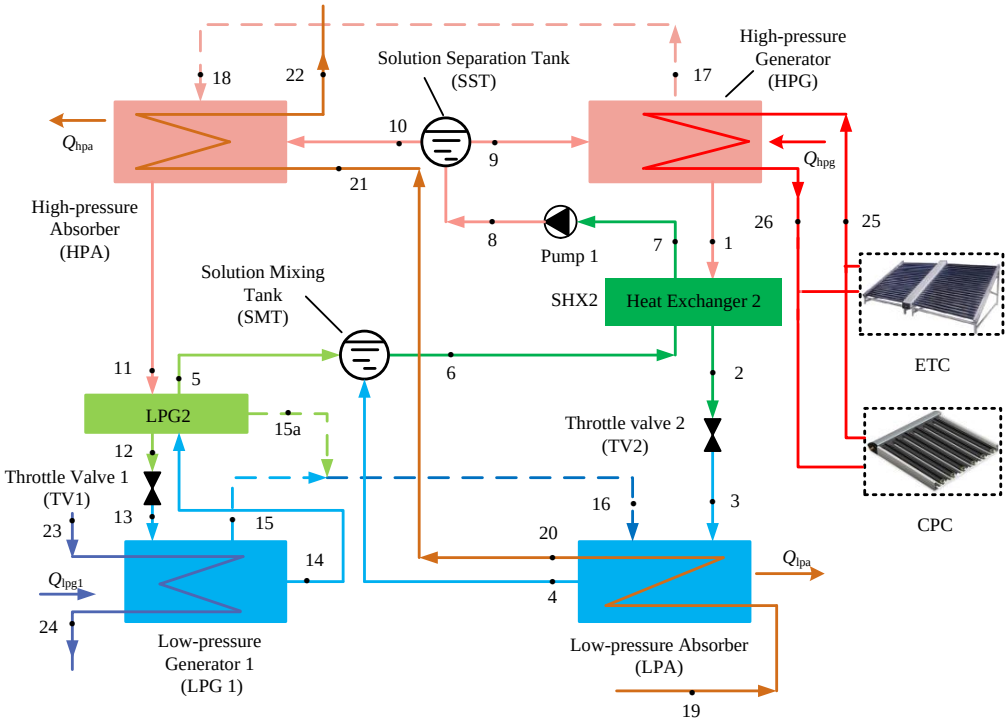

Fig. 2: Schematic diagram of the novel ARHP cycle

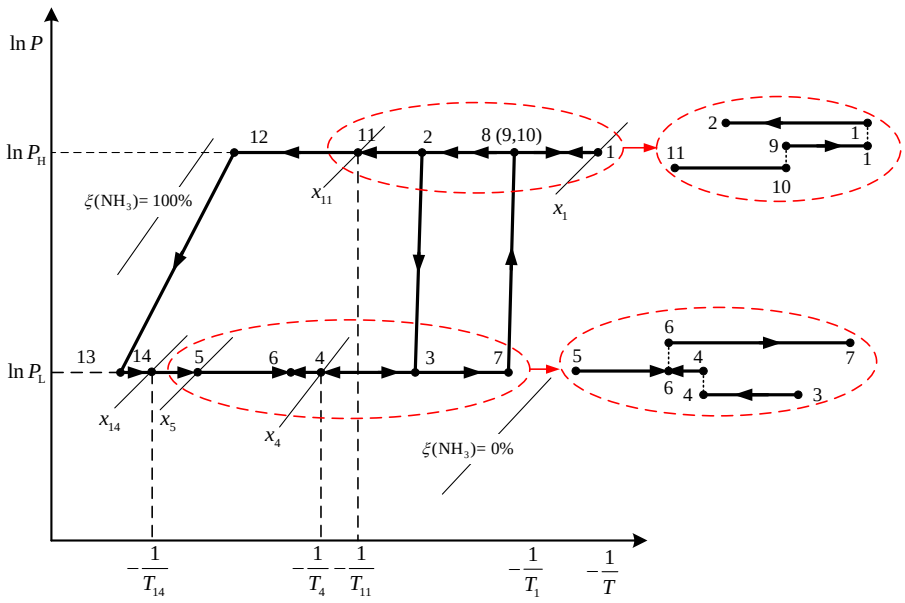

Fig. 3: *P-T* diagram of the novel ARHP cycle

3. Mathematical model

In this paper, low-temperature solar thermal of about 80℃-100℃ works as the high-temperature heat source. A mathematical model is developed to analyze the performance of the proposed cycle. Performance of the proposed cycle is simulated and compared to conventional single-stage cycle. The model can be simplified by the following assumptions:

(1) The system runs in a steady state;

(2) Heat losses to the surroundings and pressure drops along the pipelines are neglected;

(3) The solutions out from the LPG, HPG, LPA and HPA are all saturated;

(4) The vapor out from the LPG and HPG are saturated;

(5) The process in the solution pump is adiabatic.

(6) The expansion processes in throttling valves are isenthalpic.

(7) The mixing process in the solution mixing tank is adiabatic.

The proposed cycle comprises several relatively simple components such as the solution pump, heat exchangers, solution mixing tank, valves, and solution separation tank, HPG, LPG (1 and 2), HPA and LPA. Each component can be taken as a control volume with inlet and outlet fluid, heat transfer and work interactions (Hong 2011). The basic models for all of the components include energy balance equation, solution mass balance equation and ammonia mass balance equation, which are shown respectively as follows in Table 1.

ab. 1: Basic equations of the main components in the heat pump cycle

Components	Balance equations	
HPG	$m_9 h_9 + Q_{hpg} = m_1 h_1 + m_{17} h_{17}$	(eq. 1)
	$m_9 = m_1 + m_{17}$	(eq. 2)
	$m_9 x_9 = m_1 x_1 + m_{17} x_{17}$	(eq. 3)
SHX2	$m_1 h_1 + m_6 h_6 = m_2 h_2 + m_7 h_7$	(eq. 4)
	$m_1 = m_2$	(eq. 5)
	$m_1 x_1 = m_2 x_2$	(eq. 6)
	$m_6 = m_7$	(eq. 7)
TV2	$m_2 h_2 = m_3 h_3$	(eq. 8)
	$m_2 = m_3$	(eq. 9)
	$m_2 x_2 = m_3 x_3$	(eq. 10)
LPA	$m_3 h_3 + m_{16} h_{16} = m_4 h_4 + Q_{lpa}$	(eq. 11)
	$m_4 = m_3 + m_{16}$	(eq. 12)
	$m_4 x_4 = m_3 x_3 + m_{16} x_{16}$	(eq. 13)
SMT	$m_5 h_5 = m_4 h_4 + m_{14} h_{14}$	(eq. 14)
	$m_5 = m_4 + m_{14}$	(eq. 15)
	$m_5 x_5 = m_4 x_4 + m_{14} x_{14}$	(eq. 16)
LPG1	$m_{13} h_{13} + Q_{lpg1} = m_{14} h_{14} + m_{15} h_{15}$	(eq. 17)
	$m_{13} = m_{14} + m_{15}$	(eq. 18)
	$m_{13} x_{13} = m_{14} x_{14} + m_{15} x_{15}$	(eq. 19)
TV1	$m_{12} h_{12} = m_{13} h_{13}$	(eq. 20)
	$m_{12} = m_{13}$	(eq. 21)
	$m_{11} h_{11} + m_5 h_5 = m_{12} h_{12} + m_6 h_6$	(eq. 22)
SHX1	$m_{11} = m_{12}$	(eq. 23)
	$m_{11} x_{11} = m_{12} x_{12}$	(eq. 24)
	$m_6 = m_5$	(eq. 25)
	$m_6 x_6 = m_5 x_5$	(eq. 26)
	$m_{10} h_{10} + m_{17} h_{17} = m_{11} h_{11} + Q_{hpa}$	(eq. 27)

HPA	$m_{11}x_{11} = m_{10}x_{10} + m_{17}x_{17}$	(eq. 28)
	$m_{11} = m_{10} + m_{17}$	(eq. 29)
P1	$m_7h_7 + W_{p1} = m_8h_8$	(eq. 30)
	$m_7 = m_8$	(eq. 31)
	$m_7x_7 = m_8x_8$	(eq. 32)
SST	$m_8h_8 = m_9h_9 + m_{10}h_{10}$	(eq. 33)
	$m_8 = m_9 + m_{10}$	(eq. 34)
	$m_8x_8 = m_9x_9 + m_{10}x_{10}$	(eq. 35)
LPG2	$m_{14}h_{14} + m_{11}h_{11} = m_{12}h_{12} + m_5h_5 + m_{15a}h_{15a}$	(eq. 36)
	$m_{14} = m_5 + m_{15a}$	(eq. 37)
	$m_{14}x_{14} = m_5x_5 + m_{15a}x_{15a}$	(eq. 38)

In this paper, COP is adopted to evaluate performance of the proposed NH_3-H_2O absorption-resorption cycle. It can be defined as heating capacity output divided by the total energy input, given by

$$COP = \frac{Q_{hpa} + Q_{lpa}}{Q_{hpg}} = 1 + \frac{Q_{lpg1}}{Q_{hpg}} \quad \text{(eq. 39)}$$

Where Q_{lpg1} and Q_{hpg} are the total heat input of LPG1 and HPG, respectively.

All the properties of ammonia-water and pure ammonia are calculated by the REFPROP 8.0.

4. Results and discussion

In this paper, all the simulation results are based on the assumption that mass flow rate of low-pressure refrigerant vapor is 0.034 kg/s, i.e. m_{16} = 0.034 kg/s. The initial working conditions are listed in Table 2.

Tab. 2 Initial working condition

Working conditions	Given values (°C)
Temperature of solution out from HPG (1)	90
Temperature of solution out from HPA (11)	40
Temperature of solution out from LPA (4)	35
Temperature of the return water (19)	30
Ambient air temperature	10
Temperature difference between ambient air and solution (14)	3
Cold end temperature difference of SHX2, i.e. $T_2 - T_6$	10
Temperature difference between HTF outlet and solution (1), $T_{25} - T_1$	5
Temperature difference in LPG2, i.e. $T_5 - T_{14}$	5

Performance of the proposed cycle has been simulated under working conditions listed in Table 2. Simulation results are illustrated in Figs. 4-8.

Fig. 4 shows the effect of P_H (high generation pressure) values and P_L (low generation pressure) values on COP of the novel cycle. It can be seen that for a given P_H value, the COP increases rapidly with the increasing of P_L at first and then decreases with the increasing of P_L value. Under given working conditions, each P_H value corresponds to an optimum P_L to make the cycle's COP to its maximum value. The optimum P_L value increase with the increasing of P_H value, and so does the maximum value of COP. For instance, the maximum COP values for P_H values of 0.80 MPa, 0.90 MPa, 1.00 MPa, 1.10 MPa, 1.20 MPa, 1.30 MPa and 1.40 MPa are 1.17, 1.20, 1.23, 1.26, 1.31, 1.36, 1.42, respectively, and the corresponding optimum P_L values are 0.18 MPa, 0.21 MPa, 0.24 MPa, 0.28 MPa, 0.31 MPa, 0.36 MPa and 0.41 MPa, respectively. For a given P_H value, the corresponding P_L value is limited in a certain range and the proposed heat pump cycle will not work beyond that range.

Fig. 5 depicts effect of P_H and P_L values on ΔT_1 of LPG1, ΔT_2 of LPA, ΔT_3 of HPG and ΔT_4 of HPA. It can be seen that ΔT_1, ΔT_2 and ΔT_4 decreases while ΔT_3 increases with the increasing of P_L value within its range. It indicates that when P_L increases, the amount of heat needed to drive the high-pressure generation process

increases.

Fig. 6 describes heat source temperature (T_{hs}) corresponding to different P_H and P_L values. It can be seen that for given P_H value, T_{hs} increases with the increasing of P_L value. It is also obvious that the maximum T_{hs} of the cycle under given working conditions reaches 51.0 °C when P_H and P_L are with the value of 0.80 MPa and 0.22 MPa, respectively, where the cycle's COP is 1.114. It can basically meet the temperature demand of winter hot water supply. It is worth mentioning that, when the cycle is operated at its maximum COP (1.42) when P_H and P_L are 1.40 MPa and 0.41 MPa, respectively, T_{hs} can still reach 43.7 °C, which can meet the temperature demand of building floor heating. Furthermore, for other selected P_H/P_L values such as 1.30/0.36 MPa, 1.20/0.31 MPa, 1.10/0.28 MPa, 1.00/0.24 MPa, 0.90/0.21 MPa and 0.80/0.18 MPa the T_{hs} values are 44.1 °C, 44.3 °C, 45.2 °C, 45.4 °C, 46.1 °C and 46.7 °C, which are all suitable for fan coil heating.

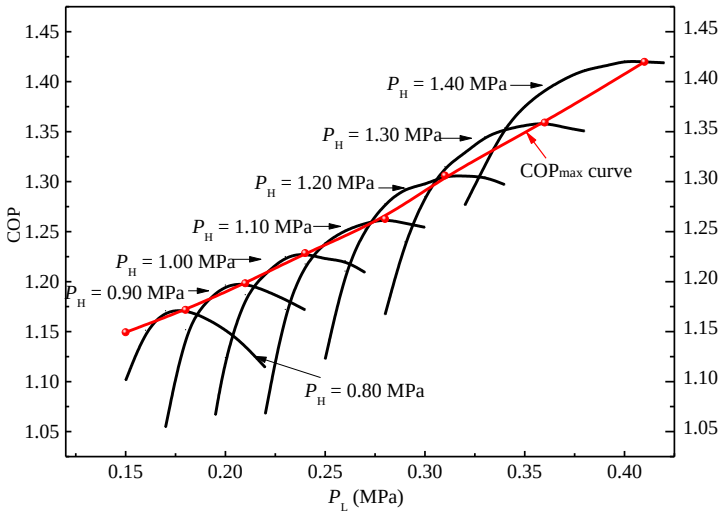

Fig. 4: The effect of P_H and P_L values on COP

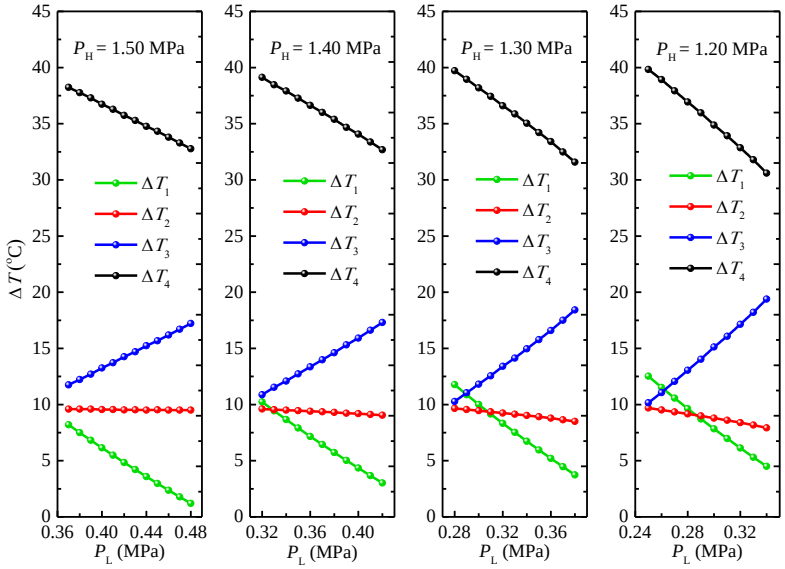

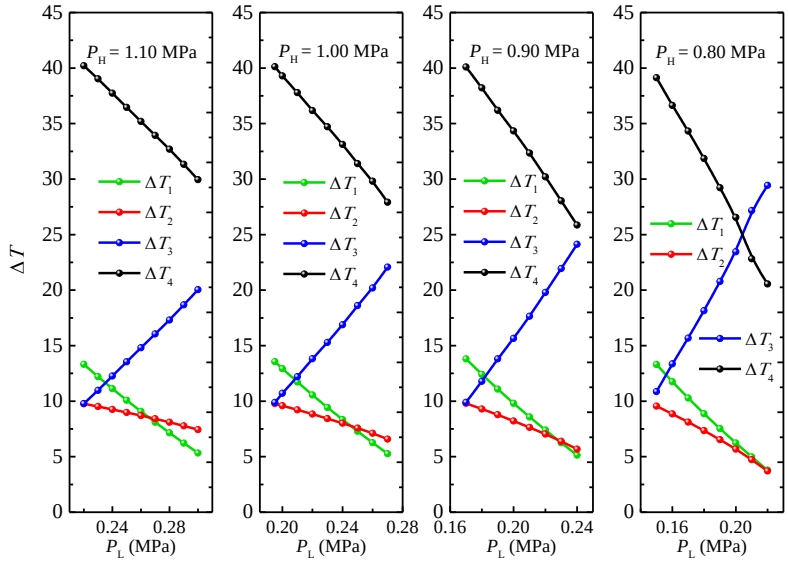

Fig. 5: Effect of P_H and P_L values on ΔT_1 of LPG1, ΔT_2 of LPA, ΔT_3 of HPG and ΔT_4 of HPA

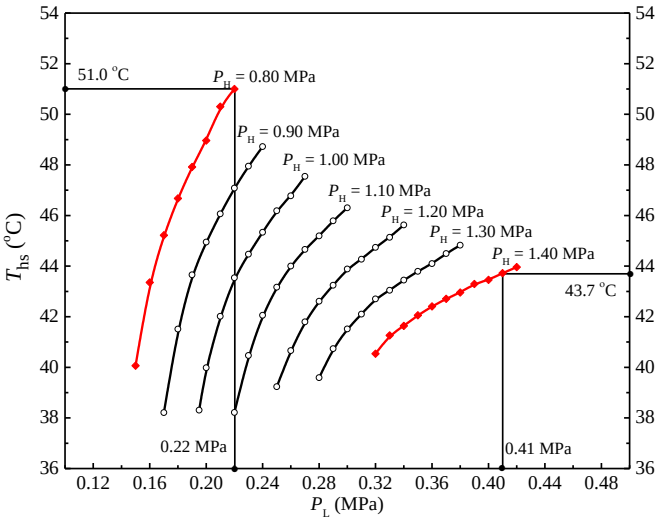

Fig. 6 Heat supply temperature (T_{hs}) corresponding to different P_H and P_L values

Fig. 7 depicts the effect of heat source temperature (T_h) on COP under the P_H/P_L pair values corresponding to the maximum COPs obtained in Fig. 4. It can be found that for the novel balanced ARHP cycle, T_h must be above 85 °C which happens when P_H/P_L pair value is 1.40/0.41 MPa and the corresponding COP value is 1.17. Meanwhile, For given P_H/P_L pair, COP firstly ascends rapidly with the increasing of T_h, and then increases slowly when T_h is higher than 95 °C. The maximum COP under given working conditions can reach 1.425.

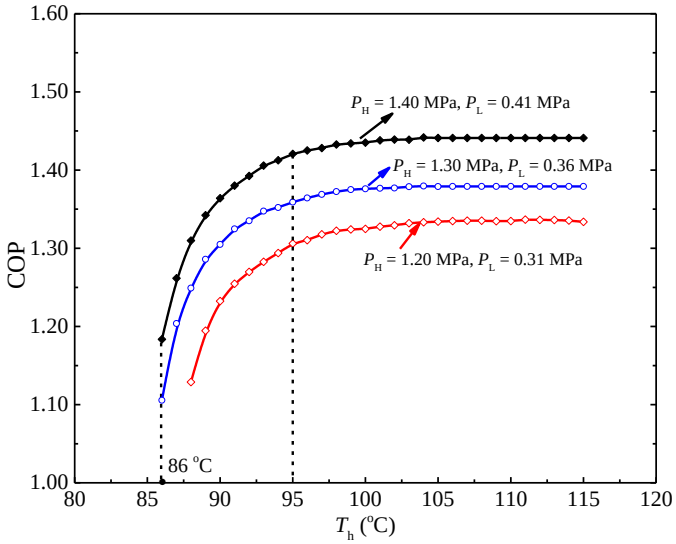

Fig. 7: Effect of heat source temperature (T_h) on COP

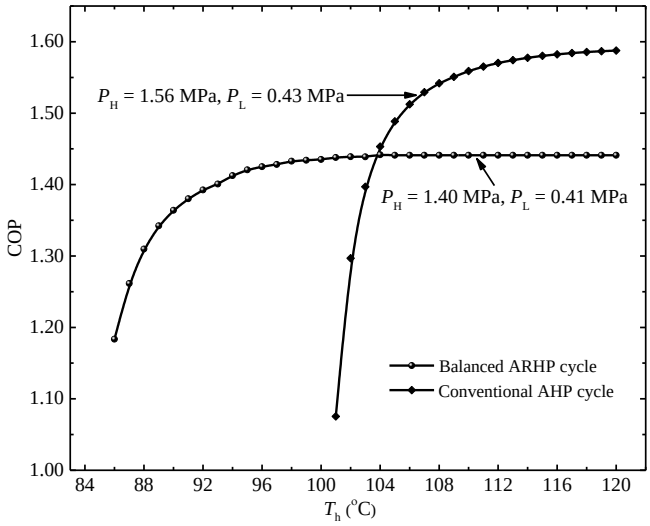

Fig. 8 Comparison of the novel ARHP cycle and the conventional AHP cycle

For comparison, effect of T_h value on COP of the conventional AHP cycle when T_e, T_c, T_a are 0 °C, 40 °C, 48 °C, respectively, and effect of T_h value on COP are also illustrated in Fig. 8. For the conventional AHP cycle, T_h must be higher than 101 °C, and when T_h is higher than 104 °C, COP of the balanced ARHP cycle is lower than that of the conventional AHP cycle. However, COP of the conventional AHP cycle declines quickly when T_{hd} is lower than 108 °C. Furthermore, the AHP cycle will stop working whereas the balanced ARHP cycle could still operate when T_h is lower than 100 °C. Apparently, the balanced ARHP cycle we proposed could function under a larger heat source temperature range than the conventional AHP cycle.

5. Summary and conclusions

To make efficient use of low-temperature solar thermal, this paper proposes a novel absorption-resorption heat pump cycle. The new resorption heat pump cycle without distillation device is more suitable for temperature characteristics of the solar heat source. Parameters like the pressure of the cycle, heat source temperature and heat supply temperature are investigated. COP of the novel cycle in this paper can reach up to 1.42 with low temperature of solar thermal acting as the high-temperature heat source. P_H and P_L value are important on the performance of the heat pump cycle. Pressure of the high-pressure generator and pressure of the low-pressure generator could be optimized to get a maximum COP at any given working conditions. The novel cycle can supply water that can meet space heating temperature demand.

Multiple heat sources with different temperatures can also be efficiently used at the same time by slightly modifying the configuration of the cycle. And when the ambient temperature is too low to drive the cycle, solar thermal collectors can be used to lift the temperature in the low-pressure generator.

References

Chua, K.J., Chou, S.K., Yang W.M., 2010. Advances in heat pump systems: A review. Appl. Energy. 87(12), 3611-3624.

Fatouh, M., Elgendy, E., 2011. Experimental investigation of a vapor compression heat pump used for cooling and heating applications. Energy. 36(5), 2788-2795.

Fraga, C., Mermoud F., Hollmuller P., et al., 2015. Large solar driven heat pump system for a multifamily building: Long term in-situ monitoring. Solar Energy. 114, 427-439.

Jradi, M., Veje, C., Jørgensen, B.N., 2017. Performance analysis of a soil-based thermal energy storage system using solar-driven air-source heat pump for Danish buildings sector. Appl. Therm. Eng. 114, 360-373.

Zhou, J., Zhao, X., Ma, X., et al., 2016. Experimental investigation of a solar driven direct-expansion heat pump system employing the novel PV/micro-channels-evaporator modules. Appl. Energy. 178, 484-495.

Dai, Y.J., Li, X., Wang, R.Z., 2015. Theoretical analysis and case study on solar driven two-stage rotary desiccant cooling system combined with geothermal heat pump. Energy Procedia. 70, 418-426.

Ozcan, H., Dincer, I., 2013. Exergy Analysis and Environmental Impact Assessment of Solar-Driven Heat Pump Drying Systems, Causes. Impacts and Solutions to Global Warming. New York, 839-858.

Omojaro, P., Breitkopf, C., 2013. Direct expansion solar assisted heat pumps: A review of applications and recent research. Renew. Sust. Energy Rev. 22, 33-45.

Wu, W., Wang, B., Shi, W., et al., 2014a. Absorption heating technologies: a review and perspective. Appl. Energy. 130, 51-71.

Wu, W., Wang, B., Shi, W., et al., 2014b. An overview of ammonia-based absorption chillers and heat pumps. Renew. Sust. Energy Rev. 31, 681-707.

Van de Bor, D.M., Ferreira, C.A.I., Kiss, A.A., 2014. Optimal performance of compression–resorption heat pump systems. Appl. Therm. Eng. 65(1),219-225.

Velázquez, N., Best, R., 2002. Methodology for the energy analysis of an air cooled GAX absorption heat pump operated by natural gas and solar energy. Appl. Therm. Eng. 22(10),1089-1103.

Du, K., Yang, S.W., Zhang, S.Q., 1991. Experimental analysis and research of an aqua ammonia absorption-resorption heat pump, J. Eng. Thermophys. 3(12), 229-233 (in Chinese).

Du, K., Yang, S.W., Zhang, S.Q., 1993. Performance simulation and analysis of aqua ammonia absorption-resorption heat pump, J. Southeast Univ. 2(23), 26-32 (in Chinese).

Hong, D.L., Chen, G.M., Tang, L.M., et al, 2011. Simulation research on an EAX (Evaporator-Absorber-Exchange) absorption refrigeration cycle. Energy. 36(1), 94-98.

NIST Reference Fluid Thermodynamic and Transport Properties Database (REFPROP): Version 8.0.